

Published in final edited form as:

J Mol Biol. 2012 October 12; 423(1): 1–13. doi:10.1016/j.jmb.2012.06.033.

Mass spectrometry - From peripheral proteins to membrane motors

Nina Morgner¹, Felipe Montenegro², Nelson P Barrera², and Carol V Robinson¹

¹Department of Chemistry, South Parks Road, University of Oxford, OX1 5QY, UK

²Department of Physiology, Pontificia Universidad Católica de Chile, Alameda 340, Santiago, 8331150, Chile

Abstract

That membrane protein complexes could survive in the gas phase had always seemed impossible. The lack of chargeable residues, high hydrophobicity, poor solubility and the vast excess of detergent contributed to the view that it would not be possible to obtain mass spectra of intact membrane complexes. With the recent success in recording mass spectra of these complexes, first from recombinant sources and later from the cellular environment, many surprising properties of these gas phase membrane complexes have been revealed. The first of these was that the interactions between membrane and soluble subunits could survive in vacuum, without detergent molecules adhering to the complex. The second unexpected feature was that their hydrophobicity, and consequently lower charge state, did not preclude ionization. The final surprising finding was that these gas phase membrane complexes carry with them lipids, bounds specifically in subunit interfaces. This provides us with an opportunity to distinguish annular lipids that surround the membrane complexes, from structural lipids that have a role in maintaining structure and subunit interactions. In this review we track these developments and suggest explanations for the various discoveries made during this research.

Introduction

The electrospray MS of individual proteins was first described in 1989¹. More than two decades later, and after many intact soluble complexes have been transmitted into the gas phase^{2; 3; 4} it has finally become possible to ‘fly’ an intact membrane embedded motor⁵. Given the very high concentrations of detergent necessary to maintain the solubility of these complexes, and the hydrophobic nature of the interactions between membrane subunits, such an observation had seemed unattainable. Two ionization methods have been successfully employed for the MS of intact membrane complexes: electrospray (ES) and laser-induced liquid bead ion desorption (LILBID). In this review we trace the developments that have made application of these two techniques possible and show how studying intact rotary motors in the gas phase, using either LILBID or ES, is shedding new light on subunit stoichiometry in membrane complexes. In the case of ES, it has also been possible to demonstrate specific lipid binding. We discuss the implications of this finding and show how this information led to proposals for the regulation and control of the membrane embedded complexes in two different rotary motors⁵.

The challenge of membrane proteins

In their native state membrane proteins are embedded in a lipid bilayer, which shields the transmembrane subunits from water. For a solvated membrane protein the role of the bulk membrane lipids has to be replaced by detergents, which are added at relatively high concentrations to the buffer solution to form micelles. While high concentrations of detergent can be tolerated in the LILBID approach, from an ES MS viewpoint the presence of detergent leads to suppression of the membrane protein spectrum⁶. In addition, poor solubility of membrane proteins, the lack of charged residues and the hydrophobic nature of the interactions between membrane subunits, had long been assumed to make membrane complexes unsuitable for investigation by ES. The detergent background necessitates the use of high activation in the gas phase to obtain well-resolved charge states for the protein complex. An additional impediment for resolution was the possibility of multiple lipids adhering tightly to the protein complex. These lipid-binding properties were for example cited as a reason for the absence of the tetrameric state in initial attempts to obtain mass spectra of the intact of the K⁺ channel KcsA⁷. The harsh MS conditions that were necessary to strip lipids and detergents resulted in observation of dissociated KcsA subunits only.

First steps – transmembrane peptides and peripheral proteins

Given these results for protein assemblies, it was necessary to step back and to start with simple transmembrane peptides. Results from these studies were encouraging. Mass spectra, combined with hydrogen exchange methods, indicated that folded peptide backbone could be preserved in the gas phase^{8; 9}. These prompted further experiments to investigate the lipid environment surrounding a single transmembrane helix. Using UV activation of a photoactivatable cross-linker, neighbouring lipids were cross-linked to a model transmembrane peptide and identified by MS¹⁰. Interestingly the anticipated molecular sorting of the lipids around the peptide, based on hydrophobic matching, was not observed. These results imply that hydrophobic matching is more likely to be associated with increased rigidity of multispinning proteins, as opposed to the single transmembrane helix (TMH) that was investigated.

While it was possible to obtain ES spectra of transmembrane peptides^{8; 9}, at this stage it seemed that the goal of obtaining well-resolved mass spectra of integral membrane protein complexes would be compromised by the presence of tightly bound lipids and excess detergent. We therefore selected a peripheral membrane protein, *apo* lipoprotein C-II, a phospholipid binding protein that binds on the surface of plasma lipoproteins¹¹. We first examined interactions between phospholipids in the absence of *apo* lipoprotein C-II¹², demonstrating that it was possible to maintain clusters with ~80 phospholipids. Interactions between the protein and phospholipids however were restricted to between 5 and 10 lipid molecules. Interestingly we noted that in a suspension of two different phospholipids without protein, lipids with the same headgroup self-associated rather than forming mixed aggregates¹². When *apo* lipoprotein C-II was added to this mixed lipid environment however, self-association was perturbed, in favour of a statistical distribution of lipids bound to *apo* lipoprotein C-II. This re-distribution indicated that lipid interactions with *apo* lipoprotein C-II are dominant, prompting the conclusion that the protein is capable of

remodelling the lipid environment. This was an encouraging result since it implied that MS could be used to investigate specific protein lipid interactions, in the absence of crosslinking, at least for peripheral membrane proteins.

First mass spectra of integral membrane proteins reveal interfacial lipid binding

First attempts to investigate integral membrane protein complexes focussed on the multidrug transporter EmrE. Electron cryomicroscopy of 2D crystals of this protein had shown that it forms an asymmetric dimer with eight transmembrane helices (TMH) forming a drug-binding pocket for one substrate molecule near the centre¹³. Crystals of EmrE were formed in the presence of the substrate TPP⁺ since addition of the ligand produced more ordered crystals than the protein alone. The drug transport mechanism was rationalised by binding of the substrate to the binding pocket, a conformational change of the dimer, which opens the binding chamber to the periplasm. This is followed by binding of one proton, displacing the substrate and of a second which induces a conformational change back to the original position. The role of lipids in this mechanism and their specific binding could not be assessed at the 7 Å resolution obtained in this study.

Since there was excellent evidence for the dimeric form of EmrE and given its relatively small size we reasoned that the dimensions of the associated detergent micelle would also be relatively minor¹⁴ and consequently the ratio of detergent to protein could be favourable for ES. We introduced this protein into the gas phase with the ligand (TPP⁺), used to obtain ordered crystals, and removed large proportions of the detergent from the solution prior to analysis¹⁵. We hypothesised that two dissociation pathways were possible (figure 1). Pathway [1] in which the micelle complex dissociates upon activation in the gas phase and interactions between the protein subunits are lost. Alternatively pathway [2], the optimal process for investigation with MS, would involve activation only of the micelle in the gas phase, enabling the subunit interactions within the protein complex to be retained.

Our first mass spectra of the EmrE complex from a DDM-containing buffered solution revealed large, heterogeneous gas phase detergent aggregates, the sizes of which were highly dependent on the pressure and accelerating voltages within the mass spectrometer (Figure 1 (i)). This occurred in spite of our attempts to remove detergent in solution. These early mass spectra of protein micelle complexes did not reveal charge states for the protein. Rather the presence of the very broad distribution of detergent and detergent-protein aggregates masked the protein peaks. A tandem MS procedure was used to isolate a narrow m/z region of this broad peak, releasing individual protein subunits as well as the TPP⁺ ligand and clusters of DDM molecules (Figure 1 (ii)). These spectra demonstrated the feasibility for screening ligands, released in mass spectra. Under these conditions however interactions between protein subunits, small molecules and lipids did not survive. This absence of subunit interactions in mass spectra was attributed to the conditions that were necessary to break up the detergent aggregates during collisional activation.

An additional reason for the lack of success in maintaining subunit interactions in EmrE we attribute to the fact that the dimer is relatively weakly associated. In the membrane the EmrE

subunit interactions are likely held in place, at least in part, by the lateral forces of the membrane and specific interactions with surrounding lipids. Extraction from the membrane with detergents, and subsequent removal of detergent prior to analysis, will destroy the protective micelles around the complex and weaken the interactions between the subunits. These subunit interactions are therefore most likely lost in the solution state, before the complex is introduced into the mass spectrometer.

Searching for a system in which protein interactions would likely be more stable in solution and gas phases than the simple EmrE dimer we turned our attention to the multidrug resistance pump Tol C (150 kDa). In this case there is a much larger interaction surface between the three Tol C protomers which form a continuous, solvent-accessible conduit over 140 Å long that spans both the outer membrane and periplasmic space¹⁶. Moreover approximately 70% of this complex is outside the membrane and is soluble. These structural properties imply that there would be sufficient charged amino acids to form electrostatic interactions to complement and strengthen the predominantly hydrophobic interactions in the membrane embedded region. Excess octylglucoside detergent was removed prior to analysis. The resulting mass spectrum gave rise to broad peaks consistent with both the trimeric and monomeric forms of the complex. Resolution of these peaks however and the intensity of the membrane complex was relatively low (figure 2 upper spectrum). The fact that the trimeric state was visible however gave us confidence that membrane protein complexes could survive. It seemed as this time, however, that this might only be possible if the majority of the protein is located outside the membrane.

In parallel to our investigations and using a similar strategy the ES mass spectrum of rat microsomal glutathione transferase-1 (MGST1) was reported¹⁷. The complex was stabilised by the addition of the substrate glutathione (GSH) prior to analysis. Weak peaks were discerned for a trimeric form of the complex as well as a monomer and dimer after introduction from a triton-containing buffered solution¹⁷. Evidence of non-covalent binding of one GSH molecule to the trimer was in accord with the proposed active form of the enzyme being homotrimeric. Lipid binding however was not observed under the MS conditions used at this time for Tol C and EmrE..

Many additional membrane complexes that were attempted could not be detected with sufficient resolution, or were not observed in one stable form. As such it was difficult to define unambiguously their oligomeric state. In order to develop a more reliable method we needed a better understanding of the properties of detergent micelles and their interaction with proteins in the gas phase.

Properties of a ‘gas phase micelle’

A typical detergent micelle in aqueous solution forms an aggregate (for DDM on average ~ 100 DDM molecules¹⁸) with the hydrophilic “head” regions of each detergent molecule in contact with the aqueous solution, sequestering the hydrophobic tail regions in the centre of the micelle. In a protein micelle complex the size of the micelle is larger than an empty detergent micelle¹⁹ but the detergents have a similar arrangement, protecting the hydrophobic areas of the protein with the hydrophobic tails of the detergent alkyl chains.

Such an environment, while capable of mimicking the hydrophobic milieu of the membrane in solution, has little or no meaning in the gas phase. The stabilising effects possessed by a detergent micelle in an aqueous solution are rapidly lost during evaporation. The high local concentration of detergent that exists following evaporation promotes formation of detergent aggregates, which hamper the analysis of protein complexes.

We began a systematic study of the properties of detergent micelles, guided by early successes with non-ionic detergents that had been shown to be suitable for study in the gas phase²⁰ for individual denatured proteins²¹ and folded peptides⁹. We selected first the CTAB detergent since it forms both normal and reverse micelles as a function of the solution conditions²². This study demonstrated that many 100s of molecules associate to form gas phase detergent aggregates. Interestingly however we observed that these aggregates, as well as a series formed from the N-TAB series of detergents²³, were unable to attain the charge states predicted by their surface area, presumably due to their instability at higher charges. Protein complexes, by contrast, remain stable with more charges than detergent aggregates^{22, 23}. Varying independently the effects of charge and alkyl chain length, and monitoring survival in the gas phase, showed that detergent aggregates with longer chains could be disrupted in the gas phase more readily than their shorter chain counterparts²³. This is contrary to solution behaviour²⁴. This implies therefore that long-chained detergents, whose stability was compromised in the gas phase, might enable protein complexes to escape detergent micelles more readily than their shorter chain counterparts. Consequently the longer alkyl chain non-ionic detergent, dodecylmaltoside, would be a better candidate for release of a membrane complex in the gas phase than its hexylmaltoside analogue.

Membrane protein complexes at last

Having optimised the detergent and MS conditions to produce micelles that were only marginally stable in the gas phase we attempted to release a protein complex from a detergent micelle. We reasoned that the real test for survival of a membrane protein complex would be the preservation of interactions between membrane and soluble subunits in a single well-defined stoichiometry. For this reason the BtuC₂D₂ heterotetramer was selected. This vitamin B12 transporter was crystallised as a tetramer containing two transmembrane (BtuC) and two soluble (BtuD) subunits²⁵. After introduction of BtuC₂D₂ in a solution containing DDM above the CMC, mass spectra revealed that the complex could be released from the micelle and all interactions between subunits in the heterotetramer could be preserved intact in the gas phase²⁶. This was an exciting result since, although the stoichiometry was well established, this was the first example of a heteromeric complex in the gas phase, its 2:2 subunit stoichiometry following ES, ruling out the possibility of non-specific associations. Moreover its trimeric dissociation products, formed above the *m/z* value of the tetramer, provided further confirmation of the intact tetramer as the predominant gas phase complex. The resolution that was achieved in the mass spectrum also enabled observation of the cooperative binding of nucleotides and the identification of post-translational modification of subunits within the complex.

A comparable proof of principle for the mass spectrometric analysis of membrane proteins with DDM above the CMC was achieved for the *bc1* complex and the cytochrome *c* oxidase from the respiratory chain using (LILBID)²⁷. The composition of both complexes was confirmed as hetero trimer and hetero tetramer respectively, again ruling out any possibility of protein aggregation. In the case of the *bc1* complex, dimeric as well as higher oligomeric structures²⁸ had been reported previously. The oligomerisation state of the *bc1* complex observed with LILBID was that of a tetramer, supporting the dimer of dimers as the active state of this complex.

Specific lipid binding - interfacial lipids?

With this new strategy of maintaining detergent concentrations well above the CMC we returned to the ES MS of the two complexes reported above (EmrE and Tol C) applying ES to these protein micelle solutions (Figs 1 and 2). For EmrE a clear dimeric form of the complex was liberated using higher collision energies than had been employed previously (Figure 1 (iv)). Comparing the spectra obtained under these different conditions is quite revealing. At low detergent concentrations the monomer is observed with 6+ charges, presumably the protein is monomeric in solution due to the absence of the micelle. The monomeric protein subunits then dissociate from the gas phase detergent aggregate following tandem MS. In contrast in solution conditions where detergent is above the CMC, a spectrum showing a 4+ monomer and an 8+ dimer was recorded. The conservation of charge between the monomeric and dimeric forms (2x4+) is consistent with a predominantly hydrophobic interaction²⁹. This is in contrast to the many instances observed in soluble complexes where charges are buried in subunit interfaces upon complex formation, leading to a lower overall charge than would be obtained from the sum of the charges on the component subunits^{30; 31}. For Tol C, introduced from a detergent micelle in solution, only the trimeric state was observed (figure 2 lower spectrum) and the average charge state was considerably reduced compared to the spectrum recorded previously. Not only was the oligomeric state now unambiguous, the resolution that could be obtained under these optimised conditions, revealed binding of up to two lipid molecules.

Having maintained these complexes intact with sufficient resolution to explore small molecule binding, this ES approach was applied to targets in advance of their X-ray structures. MexB and LmrCD, which were found to be trimeric and heterodimeric respectively²⁹, and MacB was identified as dimeric³². In all cases only one stoichiometry was apparent and the mass spectra of all three complexes revealed specific lipid binding. While it was not possible to determine directly whether or not these were annular lipids or interfacial lipids between subunits, the fact that they were present only when higher oligomers were observed, and not bound to the isolated subunits, strongly implies binding within subunit interfaces.

Interestingly while a plot of the surface area for soluble complexes against their average charge states is highly correlated the same relationship does not adhere for membrane complexes (Figure 3). To understand the origin of this difference we first need to consider the electrospray process itself. While the correlation between charge state and surface area is the subject of much ongoing research³³ it is generally accepted that the charge states in the

mass spectrum are defined during the final stages of the electrospray process. It could be envisioned therefore that the accessible surface area should include the area of the detergent micelle (upper row of structures and (i) for LmrA). A plot of the surface area of a protein micelle complex against the average charge state highlights a significant deviation from the relationship determined for soluble complexes (blue line).

Interestingly there is some variability in the plot consistent with a difference in the size of micelle. This likely arises due to the variability in the sizes of micelles that form from the detergents used to obtain the mass spectra (either dodecyl maltoside, decyl maltoside, neopentyl glycol etc calculated using the program Packmol {Martinez, 2009 #2678}). Since the micelle increases the surface area without affecting the charge states, as discussed above for nTAB micelles in the gas phase, we then considered the relationship between the total surface area of the intact protein complex without the micelle (red line, structure (ii) for LmrA). The reduction in surface area caused by removal of the micelle led to a closer correlation with the established relationship for globular proteins but a significant deviation persisted. Next we considered the possibility that the micelle might be shielding the membrane regions of the complex from charging during electrospray. We therefore computed the surface area of the complex after subtraction of the regions protected by the micelle (lower row of structures and (iii) for LmrA). This plot is closer to that deduced for soluble complexes but an offset remains (green line). Finally we investigated subtraction of the entire membrane spanning regions (LmrA structure (iv)) and calculated the surface area of only the soluble regions of the complex. This plot leads to a very close agreement with the correlation between surface area and charge observed for soluble complexes (purple line). This close agreement between the complexes with 'membrane regions subtracted' and soluble complexes implies that basic residues in transmembrane helices are not charged.

The most likely location of protonated sites was deduced from the total number of basic residues in the membrane and soluble proteins using MD simulations in vacuum. The number of charges, determined from mass spectra, was assigned to the protonation sites that maintained the most stable structures. Considering the charges that remain when these assignments are made we find that for six complexes none of the basic sites within the membrane are charged (table 1). For two trimeric complexes (MexB and MtrE) one basic site is charged per protomer. That only a very small subset of these residues is charged in the membrane regions is attributed to the fact that these sites are occluded in the tertiary structural fold. These observations imply therefore that the micelle fulfils its critical role in maintaining solubility of the transmembrane and soluble portions rather than shielding of basic sites during electrospray ionization.

First spectra of membrane motors – evidence for lipid plugs and lipid binding between subunits

Inspired by these successes with small oligomers and heterotetramers we turned our attention to perhaps our ultimate challenge to date - that of an intact membrane embedded motor. These large rotary ATPases/synthases consist of a soluble complex (the head) as well as a membrane embedded base (rotor). The number of subunits composing the membrane rotor determines the H^+ (Na^+) /ATP ratio for ATP production / consumption. The rotor

stoichiometry varies from species to species and has been subject of a number of investigations^{34; 35; 36}. It was not clear however whether these large complexes would survive in the gas phase, let alone be released from the micelle in such a way that it would be possible to determine their subunit stoichiometry or lipid binding properties.

Focussing first on the membrane rotors the determination of subunit stoichiometries for a number of F-type ATPases was achieved using LILBID MS³⁷. An interesting case was the anaerobic, acetogenic bacterium *Acetobacterium woodii*³⁸ which encodes two types of ring subunits: two identical bacterial F₀-like c subunits c₂ and c₃ with two TMHs, and an eukaryal V_O-like (c₁) with four TMHs and only one binding site. Electron microscopy of 2D crystals showed the ring to be constructed of 22 TMH. It was not clear however, if both subunits were incorporated into the ring, or if different growth conditions influence the stoichiometry and consequently the Na⁺/ATP ratio. An unambiguous stoichiometry of c₁: c_{2/3} of 1: 9 was deduced independent of the growth medium, excluding the possibility of carbon source-dependent variation. This was the first demonstration of a F_O-V_O hybrid motor, providing 10 ion-binding sites on a 22 TMH ring. While the peaks in the LILBID mass spectra are consistent with lipid binding, the resolution on the prototype instrumentation was not sufficient to define this unambiguously.

Turning our attention to the first electrospray mass spectrometry of rotary ATPases it became clear that the activation energy used to transmit soluble complexes are not suitable for obtaining mass spectra of an intact rotary ATPase. Comparing the electrospray mass spectra recorded under similar conditions, the GroEL 14-mer spectra are well-resolved while that of the ATPase from *Thermus thermophilus* cannot be discerned from the detergent aggregates (Figure 4). Increasing internal energy effects the gas phase dissociation of the GroEL 14-mer to form 13-mers and monomers (middle panel). By contrast the spectrum of the ATPase under these conditions reveals peaks for the soluble head and its dissociation products, as well as broad peaks for the membrane embedded rotor. Interestingly there are no peaks for the intact ATPase under these conditions. Further increase in the activation energy results in the disruption all of the GroEL 14-mer, only stripped complexes and monomeric subunits remain (lower panel). By contrast these conditions yield an excellent spectrum of the ATPase with no detergent adhering to the intact complex or membrane rotor and with very little dissociation of the intact 29-subunit ATPase.

Two V-type ATPases from *Thermus thermophilus* (TtATPase) and *Enterococcus hirae* (EhATPase) were particularly interesting targets for ES since both had not been characterised fully and there are as yet no X-ray structures for the entire complexes^{39; 40}. We were interested to know if it would be possible to observe lipid binding to these membrane complexes, particularly since there was previous evidence for lipid plugs in rotary ATPases from both atomic force microscopy (AFM)⁴¹ and X-ray crystallography³⁶. For the rotor cylinder of the ATP synthase from *Ilyobacter tartaricus* AFM had been used to image the central cavity and a central plug was observed protruding from one side of the ring⁴¹. Upon incubation with phospholipase C, the plug disappeared, but the appearance of the surrounding c subunit oligomer was not affected, indicating that the plug consists of phospholipids. The high resolution X-ray structure of the K ring from *E. hirae* also revealed density in the central cavity that was assigned to lipids³⁶. In this case 20 molecules of the

most prevalent lipid with C₁₆ side chains (10 1,2-dipalmitoyl-phosphatidylglycerol and 10 1,2-dipalmitoyl-glycerol moieties) were modeled into the cavity.

Despite the high level of detergent necessary to retain solubility of this complex the mass spectrum of *Tt*ATPase is remarkably well resolved under the right MS conditions (figure 4 lower). Particularly surprising was the observation of the L subunits, in complex with subunits I and C, 12 of which form the membrane ring of this nanomotor ICL₁₂. Careful measurement of this complex using the program *Massign*⁴² revealed a mass consistent with binding of six lipids and one nucleotide. Tandem mass spectra of subcomplexes containing this membrane ring revealed that multiple lipids were attached. These lipids were identified in subsequent experiments as phosphatidylethanolamine. Interestingly however not all subunits were observed with bound lipids. There were two populations of L subunits one with lipids and one without. This suggested two different lipid-binding environments. One way to account for such an observation is formation of L-dimers in the membrane rotor, occluding six lipid-binding sites between subunits in a six-fold symmetric ring. This binding of six lipids was consistent with the mass of six lipids in the intact ICL₁₂ complex and with six-fold symmetry of the membrane rotor ring suggested by an early EM study of the *Tt*ATPase⁴³ (Figure 5). This was interesting from a functional viewpoint since all V-type ATPases characterised to date have four TMHs per subunit while all F-type ATP synthases membrane subunits have only two TMHs. Specific lipid binding to six of the twelve subunits, to form six proteolipid dimers, each with four TMH, could therefore switch the function of this motor between synthesis and pumping.

In addition to the observation of six lipid binding sites we also found changes in subunit interactions in response to various external stimuli. Unexpectedly in high pH or low ATP concentrations we also observed more ready dissociation of subunit I. This at first was puzzling since regulatory mechanisms designed to close the proton channel in the separated Vo complex had evoked the theory of a tightening of this membrane channel and hence an increase in interactions between subunit I and the membrane rotor⁴⁴. Clearly this was not observed. An investigation of this complex by ion mobility MS, a method that reports on the collision cross section of protein complexes^{45 46}, revealed conformational heterogeneity as evidenced by the broad arrival time distributions⁵. A rationale consistent with this data is therefore that subunit I senses the nucleotide environment and moves away from the channel, allowing lipids in the membrane to move in to seal the gap created by this movement. This would ensure that the proton gradient, established at the expense of ATP consumption, is preserved if ATP concentrations in cells are depleted. As a further response to nucleotide concentration we noted in tandem MS that different dissociation pathways were possible from the soluble head complex. In the presence of ATP sequential loss of first subunit F and then D was observed. In the absence of ATP, or when ADP concentrations are high, concomitant loss of subunits F or D is observed. This latter scenario is consistent therefore with direct interactions between subunit F and the soluble head upon ATP depletion and further implies that F prevents free rotation of the head by a direct interaction. This observation allows us to propose a second regulatory mechanism in which free rotation of the head is prevented and ATP concentrations are therefore conserved.

Very recently a high resolution EM structure of the *Tt*ATPase was published, revealing a detailed model the membrane region⁴⁷. In comparison with our model, produced by homology modelling, EM and constrained by ion mobility⁵ close agreement is found. Particularly interesting however was the fact that the ring did not show the six-fold symmetry observed in earlier EM studies⁴³. These recent results, together with our six lipid binding sites and earlier EM study, are consistent with the *Tt*ATPase being isolated in two different conformations: the six-fold symmetric state primed for pumping seen in our study, and the 12-fold state operating as an ATP synthase seen in the recent EM data⁴⁷. The observation of these two different states is consistent with the established dual function of this rotary ATPase which acts either to synthesise ATP or to pump protons⁴⁸.

One of the powerful features of using MS to define these molecular motors is the possibility to link quantitatively the ratio of proteins to lipids via quantitative proteomics and lipidomics. Such experiments revealed the ratio of protein to lipid to be 1: 0.5 ± 0.1 and 1: 1.2 ± 0.1 in the case of *Tt*ATPase and *Eh*ATPase respectively. Ten binding sites for cardiolipins were consistent with the mass of the lipid plug and at least four different cardiolipins were identified within this plug. These cardiolipins most likely bind to the *Eh*ATPase in the central cavity allowing a significant reduction in the orifice of the rotor enabling it to grip the central shaft through these lipid ‘brushes’ (Figure 5). For the *Tt*ATPase, by contrast, the ratio of protein to lipid was consistent with substoichiometric binding determined from the intact membrane complexes, confirming the ratio of one lipid per L subunit dimer and the rotation of this dimer within the ring to form a six-fold symmetric state. Interestingly these very different lipid binding patterns reduce the central orifice of the membrane rotor to closely similar values (38 or 39 Å), consistent with the adaptation of both membrane rotors to bind to subunit C which is conserved (Figure 5).

Future perspectives

Ever since the first X-ray structures of the voltage-dependent K⁺ channels⁴⁹ the role of lipids have both fascinated and intrigued structural biologists⁵⁰. It has now become clear that many channels require the presence of lipids for function and stability⁵¹. One of the unexpected outcomes of our MS research has been the finding that specific lipid binding to membrane protein complexes is preserved in the gas phase. At the outset we had thought that all lipids would be removed, either by the detergent or in the gas phase, and if this were not the case well-resolved mass spectra would not result. The fact that specific binding lipids can be retained in defined stoichiometries, offers new insights into their effects on structure and stability. The very different lipid binding patterns observed for the two rotary ATPases examined here, and their unexpected preservation in mass spectra, suggests a rich avenue for research into the role of lipid binding in modulating the structure and function of membrane protein complexes.

From the first steps to the eventual flight of membrane complexes it has been difficult to predict the outcomes of this research. Prior to our first successes with membrane complexes it had seemed that such experiments would not be possible. We are however now in a position to move forward using the power of mass spectrometry to identify protein subunits and bound lipids simultaneously, both quantitatively and structurally, and to define more of

the natural membrane environment by judicious choice of detergent and tailoring of extraction procedures. Of particular interest is the possibility of defining drug and lipid binding and combining both aspects to establish synergies between small molecule binding events. MS has already played a major role in defining post-translational modifications in individual proteins and is making further headway in defining their effects on interactions in soluble complexes⁵². Employing these approaches to membrane complexes suggests the possibility of unravelling their effects, not only on subunit interactions but also on the role of specific lipid and nucleotide binding sites.

Acknowledgments

We acknowledge with thanks funding from the EU councils 7th Framework PROSPECTS, an ERC advanced grant, Royal Society Professorship and Wellcome Trust Programme grant to CVR. Funding from Fondo Nacional de Desarrollo Científico y Tecnológico (FONDECYT) regular grants #1100515, #1120169 and Millennium Nucleus P10-035-F to NPB. We also acknowledge with thanks many fruitful discussions with past and present members of the CVR research group.

References

1. Fenn JB, Mann M, Meng CK, Wong SF, Whitehouse CM. Electrospray ionization for mass spectrometry of large biomolecules. *Science*. 1989; 246:64–71. [PubMed: 2675315]
2. Loo JA. Studying Noncovalent Protein Complexes by Electrospray Ionization Mass Spectrometry. *Mass Spectrom Rev*. 1997; 16:1–24. [PubMed: 9414489]
3. Rostom AA, Robinson CV. Disassembly of intact multiprotein complexes in the gas phase. *Curr Opin Struct Biol*. 1999; 9:135–41. [PubMed: 10047587]
4. Heck AJR, van den Heuvel RHH. Investigation of Intact Protein Complexes by Mass Spectrometry. *Mass Spectrom Rev*. 2004; 23:368–389. [PubMed: 15264235]
5. Zhou M, Morgner N, Barrera NP, Politis A, Isaacson SC, Matak-Vinkovic D, Murata T, Bernal RA, Stock D, Robinson CV. Mass spectrometry of intact V-type ATPases reveals bound lipids and the effects of nucleotide binding. *Science*. 2011; 334:380–5. [PubMed: 22021858]
6. Rundlett KL, Armstrong DW. Mechanism of Signal Suppression by Anionic Surfactants in Capillary Electrophoresis-Electrospray Ionization Mass Spectrometry. *Anal. Chem*. 1996; 68:3493–3497. [PubMed: 21619282]
7. Demmers JA, van Dalen A, de Kruijff B, Heck AJ, Killian JA. Interaction of the K⁺ channel KcsA with membrane phospholipids as studied by ESI mass spectrometry. *FEBS Lett*. 2003; 541:28–32. [PubMed: 12706814]
8. Bouchard M, Benjamin DR, Tito P, Robinson CV, Dobson CM. Solvent effects on the conformation of the transmembrane peptide gramicidin A: insights from electrospray ionization mass spectrometry. *Biophys J*. 2000; 78:1010–7. [PubMed: 10653814]
9. Demmers JA, Haverkamp J, Heck AJ, Koeppe RE 2nd, Killian JA. Electrospray ionization mass spectrometry as a tool to analyze hydrogen/deuterium exchange kinetics of transmembrane peptides in lipid bilayers. *Proc Natl Acad Sci U S A*. 2000; 97:3189–94. [PubMed: 10725361]
10. Ridder AN, Spelbrink RE, Demmers JA, Rijkers DT, Liskamp RM, Brunner J, Heck AJ, de Kruijff B, Killian JA. Photo-crosslinking analysis of preferential interactions between a transmembrane peptide and matching lipids. *Biochemistry*. 2004; 43:4482–9. [PubMed: 15078094]
11. Mahley RW, Innerarity TL, Rall SC Jr, Weisgraber KH. Plasma lipoproteins: apolipoprotein structure and function. *J Lipid Res*. 1984; 25:1277–94. [PubMed: 6099394]
12. Hanson CL, Ilag LL, Malo J, Hatters DM, Howlett GJ, Robinson CV. Phospholipid complexation and association with apolipoprotein C-II: insights from mass spectrometry. *Biophys J*. 2003; 85:3802–3812. [PubMed: 14645070]
13. Ubarretxena-Belandia I, Baldwin JM, Schuldiner S, Tate CG. Three-dimensional structure of the bacterial multidrug transporter EmrE shows it is an asymmetric homodimer. *Embo J*. 2003; 22:6175–81. [PubMed: 14633977]

14. Korkhov VM, Tate CG. An emerging consensus for the structure of EmrE. *Acta Crystallogr D Biol Crystallogr*. 2009; 65:186–92. [PubMed: 19171974]
15. Ilag LL, Ubarretxena-Belandia I, Tate CG, Robinson CV. Drug binding revealed by tandem mass spectrometry of a protein-micelle complex. *J Am Chem Soc*. 2004; 126:14362–3. [PubMed: 15521749]
16. Koronakis V, Sharff A, Koronakis E, Luisi B, Hughes C. Crystal structure of the bacterial membrane protein TolC central to multidrug efflux and protein export. *Nature*. 2000; 405:914–9. [PubMed: 10879525]
17. Lenggqvist J, Svensson R, Evergren E, Morgenstern R, Griffiths WJ. Observation of an intact noncovalent homotrimer of detergent-solubilized rat microsomal glutathione transferase-1 by electrospray mass spectrometry. *J Biol Chem*. 2004; 279:13311–6. [PubMed: 14726533]
18. Seddon AM, Curnow P, Booth PJ. Membrane proteins, lipids and detergents: not just a soap opera. *Biochim Biophys Acta*. 2004; 1666:105–17. [PubMed: 15519311]
19. Moller JV, le Maire M. Detergent binding as a measure of hydrophobic surface area of integral membrane proteins. *J Biol Chem*. 1993; 268:18659–72. [PubMed: 8395515]
20. Siuzdak G, Bothner B. Gas-phase micelles. *Angew Chem Int Ed Engl*. 1995; 34:2053–2055.
21. Loo RR, Dales N, Andrews PC. Surfactant effects on protein structure examined by electrospray ionization mass spectrometry. *Protein Sci*. 1994; 3:1975–83. [PubMed: 7703844]
22. Sharon M, Ilag LL, Robinson CV. Evidence for micellar structure in the gas phase. *J Am Chem Soc*. 2007; 129:8740–6. [PubMed: 17585761]
23. Martinez L, Andrade R, Birgin EG, Martinez JM. PACKMOL: a package for building initial configurations for molecular dynamics simulations. *J Comput Chem*. 2009; 30:2157–64. [PubMed: 19229944]
24. Andersen KK, Otzen DE. How chain length and charge affect surfactant denaturation of acyl coenzyme A binding protein (ACBP). *J Phys Chem B*. 2009; 113:13942–52. [PubMed: 19788195]
25. Locher KP, Lee AT, Rees DC. The E. coli BtuCD structure: a framework for ABC transporter architecture and mechanism. *Science*. 2002; 296:1091–8. [PubMed: 12004122]
26. Barrera NP, Di Bartolo N, Booth PJ, Robinson CV. Micelles protect membrane complexes from solution to vacuum. *Science*. 2008; 321:243–6. [PubMed: 18556516]
27. Morgner N, Kleinschroth T, Barth H-D, Ludwig B, Brutschy B. A novel approach to analyze membrane proteins by laser mass spectrometry: From protein subunits to the integral complex. *Journal of The American Society for Mass Spectrometry*. 2007; 18:1429–1438. [PubMed: 17544294]
28. Stroh A, Anderka O, Pfeiffer K, Yagi T, Finel M, Ludwig B, Schagger H. Assembly of Respiratory Complexes I, III, and IV into NADH Oxidase Supercomplex Stabilizes Complex I in *Paracoccus denitrificans*. *J Biol Chem*. 2004; 279:5000–5007. [PubMed: 14610094]
29. Barrera NP, Isaacson SC, Zhou M, Bavro VN, Welch A, Schaedler TA, Seeger MA, Miguel RN, Korkhov VM, van Veen HW, Venter H, Walmsley AR, Tate CG, Robinson CV. Mass spectrometry of membrane transporters reveals subunit stoichiometry and interactions. *Nature Methods*. 2009; 6:585–589. [PubMed: 19578383]
30. Rostom AA, Sunde M, Richardson SJ, Schreiber G, Jarvis S, Bateman R, Dobson CM, Robinson CV. Dissection of multi-protein complexes using mass spectrometry: subunit interactions in transthyretin and retinol-binding protein complexes. *Proteins*. 1998; (Suppl 2):3–11. [PubMed: 9849905]
31. Levy ED, Boeri-Erba E, Robinson CV, Teichmann SA. Assembly reflects evolution of protein complexes. *Nature*. 2008; 453:1262–1265. [PubMed: 18563089]
32. Lin HT, Bavro VN, Barrera NP, Frankish HM, Velamakanni S, van Veen HW, Robinson CV, Borges-Walmsley MI, Walmsley AR. MacB ABC Transporter Is a Dimer Whose ATPase Activity and Macrolide-binding Capacity Are Regulated by the Membrane Fusion Protein MacA. *J Biol Chem*. 2009; 284:1145–54. [PubMed: 18955484]
33. Hall Z, Robinson CV. Do Charge State Signatures Guarantee Protein Conformations? *J Am Soc Mass Spectrom*. 2012
34. Seelert H, Poetsch A, Dencher NA, Engel A, Stahlberg H, Muller DJ. Structural biology. Proton-powered turbine of a plant motor. *Nature*. 2000; 405:418–9. [PubMed: 10839529]

35. Pogoryelov D, Reichen C, Klyszejko AL, Brunisholz R, Muller DJ, Dimroth P, Meier T. The oligomeric state of c rings from cyanobacterial F-ATP synthases varies from 13 to 15. *J Bacteriol.* 2007; 189:5895–902. [PubMed: 17545285]
36. Murata T, Yamato I, Kakinuma Y, Leslie AG, Walker JE. Structure of the rotor of the V-Type Na⁺-ATPase from *Enterococcus hirae*. *Science.* 2005; 308:654–9. [PubMed: 15802565]
37. Meier T, Morgner N, Matthies D, Pogoryelov D, Keis S, Cook GM, Dimroth P, Brutschy B. A tridecameric c ring of the adenosine triphosphate (ATP) synthase from the thermoalkaliphilic *Bacillus* sp strain TA2.A1 facilitates ATP synthesis at low electrochemical proton potential. *Molecular Microbiology.* 2007; 65:1181–1192. [PubMed: 17645441]
38. Fritz M, Klyszejko AL, Morgner N, Vonck J, Brutschy B, Muller DJ, Meier T, Muller V. An intermediate step in the evolution of ATPases - a hybrid F₀-V₀ rotor in a bacterial Na⁺F₁F₀ ATP synthase. *Febs Journal.* 2008; 275:1999–2007. [PubMed: 18355313]
39. Lee LK, Stewart AG, Donohoe M, Bernal RA, Stock D. The structure of the peripheral stalk of *Thermus thermophilus* H⁺-ATPase/synthase. *Nat Struct Mol Biol.* 2010; 17:373–8. [PubMed: 20173764]
40. Yamamoto M, Unzai S, Saijo S, Ito K, Mizutani K, Suno-Ikeda C, Yabuki-Miyata Y, Terada T, Toyama M, Shirouzu M, Kobayashi T, Kakinuma Y, Yamato I, Yokoyama S, Iwata S, Murata T. Interaction and stoichiometry of the peripheral stalk subunits NtpE and NtpF and the N-terminal hydrophilic domain of NtpI of *Enterococcus hirae* V-ATPase. *J Biol Chem.* 2008; 283:19422–31. [PubMed: 18460472]
41. Meier T, Matthey U, Henzen F, Dimroth P, Muller DJ. The central plug in the reconstituted undecameric c cylinder of a bacterial ATP synthase consists of phospholipids. *FEBS Lett.* 2001; 505:353–6. [PubMed: 11576527]
42. Morgner N, Robinson CV. Massign: an assignment strategy for maximizing information from the mass spectra of heterogeneous protein assemblies. *Anal Chem.* 2012; 84:2939–48. [PubMed: 22409725]
43. Bernal RA, Stock D. Three-dimensional structure of the intact *Thermus thermophilus* H⁺-ATPase/synthase by electron microscopy. *Structure.* 2004; 12:1789–98. [PubMed: 15458628]
44. Muench SP, Trinick J, Harrison MA. Structural divergence of the rotary ATPases. *Q Rev Biophys.* 2011; 44:311–56. [PubMed: 21426606]
45. Ruotolo BT, Giles K, Campuzano I, Sandercock AM, Bateman RH, Robinson CV. Evidence for macromolecular protein rings in the absence of bulk water. *Science.* 2005; 310:1658–1661. [PubMed: 16293722]
46. Gill AC, Jennings KR, Wyttenbach T, Bowers MT. Conformations of biopolymers in the gas phase: a new mass spectrometric method. *Int. J. Mass Spectrom.* 2000; 196:685–697.
47. Lau WC, Rubinstein JL. Subnanometre-resolution structure of the intact *Thermus thermophilus* H⁺-driven ATP synthase. *Nature.* 2012; 481:214–8. [PubMed: 22178924]
48. Nakano M, Imamura H, Toei M, Tamakoshi M, Yoshida M, Yokoyama K. ATP hydrolysis and synthesis of a rotary motor V-ATPase from *Thermus thermophilus*. *J Biol Chem.* 2008; 283:20789–96. [PubMed: 18492667]
49. Ruta V, Jiang Y, Lee A, Chen J, MacKinnon R. Functional analysis of an archaeobacterial voltage-dependent K⁺ channel. *Nature.* 2003; 422:180–5. [PubMed: 12629550]
50. Williamson IM, Alvis SJ, East JM, Lee AG. Interactions of phospholipids with the potassium channel KcsA. *Biophys J.* 2002; 83:2026–38. [PubMed: 12324421]
51. Long SB, Tao X, Campbell EB, MacKinnon R. Atomic structure of a voltage-dependent K⁺ channel in a lipid membrane-like environment. *Nature.* 2007; 450:376–82. [PubMed: 18004376]
52. Zhou M, Robinson CV. When proteomics meets structural biology. *Trends Biochem Sci.* 2010; 35:522–9. [PubMed: 20627589]

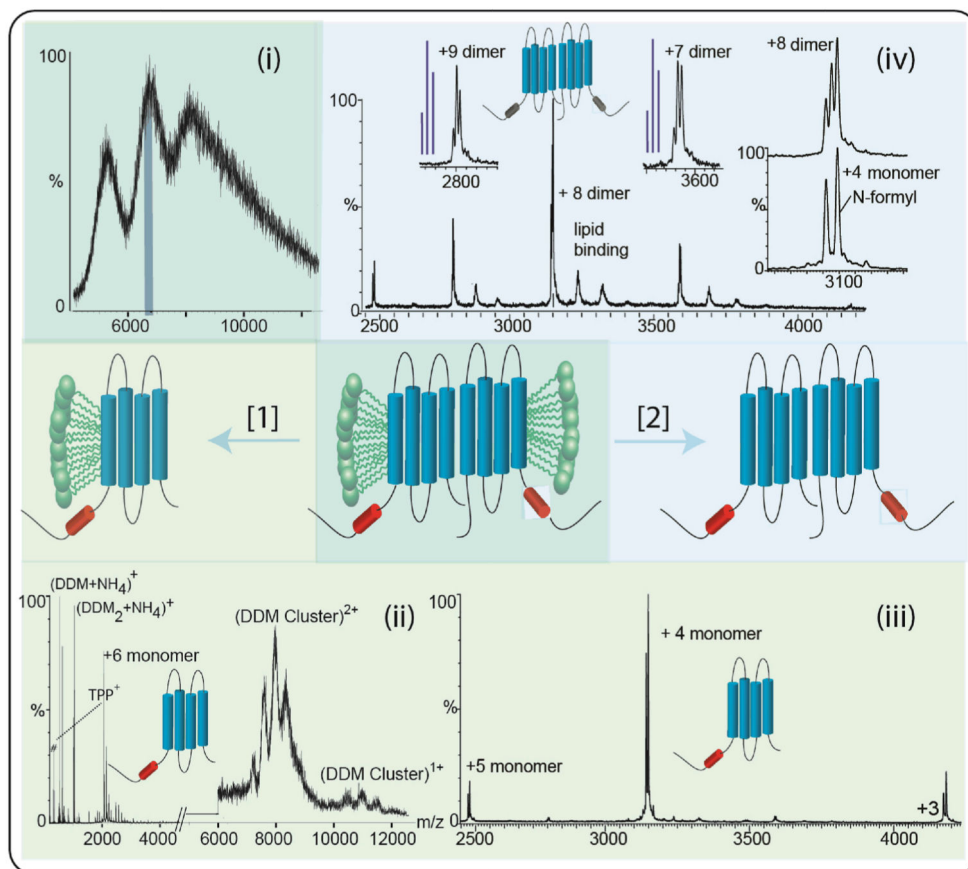


Figure 1.

Two possible dissociation pathways ([1] and [2]) of a hypothetical dimeric protein consisting of four transmembrane helices per subunit (blue) and a cytoplasmic subunit (red) in a detergent micelle (green). If the detergent concentration is depleted, activation removes detergent and disrupts subunit interactions - pathway [1] is followed. Mass spectra are shown for the membrane protein EmrE. When detergent was depleted from solution containing EmrE, prior to analysis, a broad heterogeneous distribution of detergent aggregates is formed (i). After tandem MS of a defined m/z range (blue line (i)) detergent ions, ligand (TPP^+) monomeric EmrE are observed (ii). If the detergent concentration is maintained above the CMC, and activated once in the gas phase (pathway [2]), not only is the quality of the spectra much improved (iii) but subunit interactions can also be maintained (iv). This spectrum of dimeric EmrE (iv) reveals lipid binding and PTMS (N-formyl methionine). Blue lines represent the statistical incorporation of modified and wild type subunits and are compared with data in the $+7$ and $+9$ charge states. Binding of one or two lipids is clearly observed for the protein dimer, but not for the monomer, implying that the conditions employed to preserve subunit interactions also preserve lipid binding.

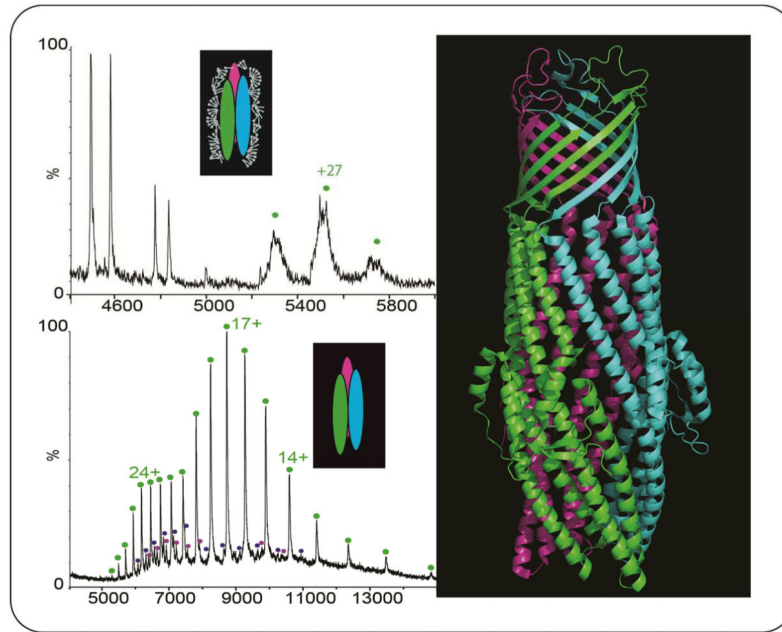


Figure 2.

Tol C was selected for study since only 30% of the protein chain is embedded in the membrane. Using a protocol whereby we buffer exchanged the octylglucoside detergent micelle into 1M ammonium acetate solution only a low proportion of the complex survived in the gas phase (upper panel). Considerable dissociation to the monomer was observed and very broad peaks for the trimer, presumably since detergent adhered to the protein subunits. By contrast, when Tol C was introduced from a DDM detergent micelle above the CMC, and when the appropriate MS conditions are employed, a well-resolved trimer is observed with one and two lipid molecules bound (purple and blue symbols).

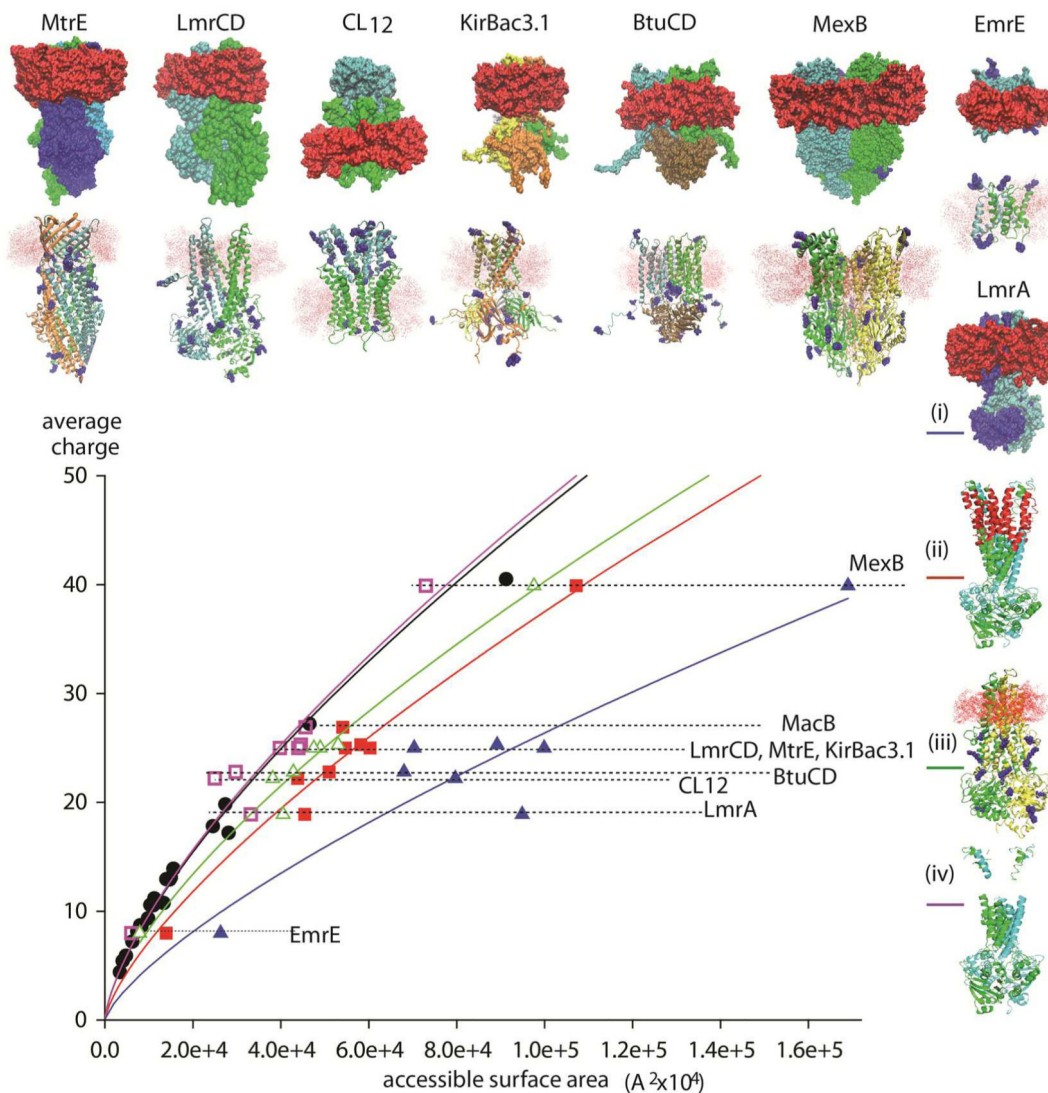


Figure 3.

Plot of the solvent accessible surface area of various membrane protein complexes and their average charge states and comparison with the analogous plot for soluble complexes (black line). Comparing the surface area of the protein micelle complexes (upper row of structures and (i) for LmrA) with the average charge state shows a deviation from the soluble complexes consistent with the contribution of the micelle to the surface area (blue line). The size and location of the micelle was calculated using the program Packmol²³. Computing the surface area of the intact protein complex without the micelle, leads to a reduction in the surface area and consequently a shift to the left (red line and structure (ii) LmrA). By subtracting the area that is protected by the micelle a closer agreement to the relationship for soluble complexes is reached (green line, lower row of structure and (iii) for LmrA). By subtracting the entire membrane spanning regions (purple line, (iv) for LmrA) and calculating the surface area of only the soluble regions of the complex, the resulting plot is virtually indistinguishable to that obtained for soluble complexes. This highlights the fact

that the membrane regions are not charged and therefore the micelle does not protect the complex from charging. Rather the charge distribution of membrane containing complexes is solely dependent on the accessible surface areas of the soluble portions.

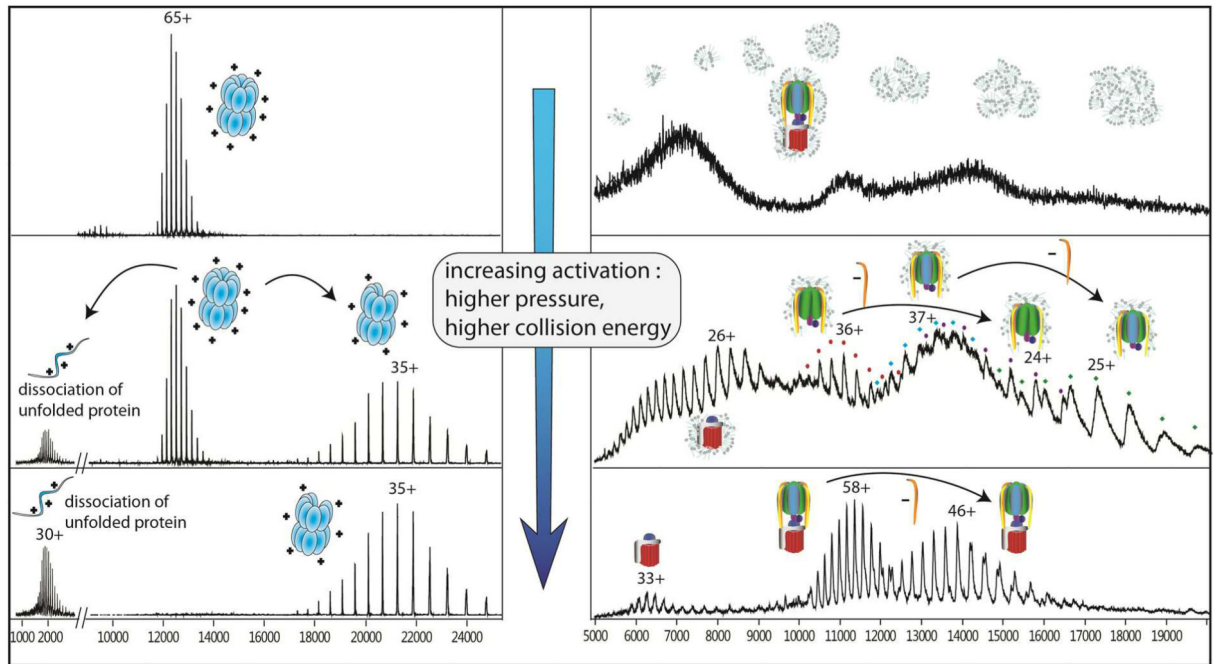


Figure 4.

Differences in behaviour of soluble and membrane complexes in the gas phase of the mass spectrometer. Mass spectra of GroEL, a soluble 14-mer (left) and the *Thermus thermophilus* ATPase, with a membrane-embedded rotor (right) under conditions of increasing activation energy. Under the lowest energy conditions (top) GroEL gives rise to a well- resolved mass spectrum, while that of the *Tt*ATPase is masked by a wide distribution of detergent aggregates. Higher activation leads to gas phase dissociation of GroEL subunits, and in the case of the ATPase, disruption of the detergent aggregates and the stripping of detergent molecules from the complex (middle). Above the detergent background, soluble subcomplexes of the ATPase head are observed. These subcomplexes are less likely to adhere to the detergent molecules. At the highest activation energies accessed, no peaks assigned to intact GroEL 14-mer remain. These conditions are however optimal for the investigation of the intact ATPase, the complex being stripped of detergent and having only one major dissociation product.

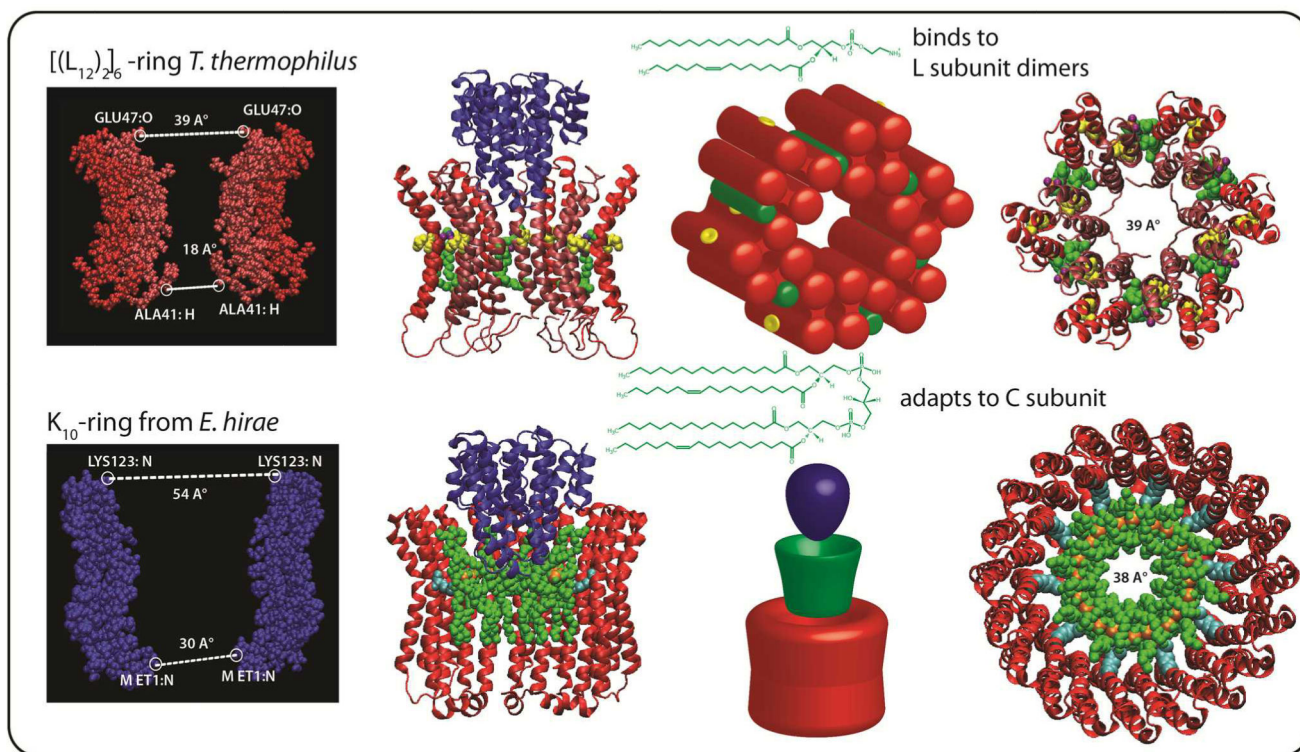


Figure 5.

Very different lipid binding patterns are observed for the two rotary ATPases examined here. In the case of *Tt*ATPase the dimensions across the widest part of the ring measured from a homology model of the L_{12} ring in which six L dimers are formed is 39 Å (based on the evolutionarily related prokaryotic *E. hirae* K subunit PDB ID: 2BL2). Lipid binding between subunit dimers is supported by quantitative lipidomics, the mass of the intact membrane complex and the observation of two populations of membrane subunits, one with tightly bound lipids and the other in its *apo* form. For *Eh*ATPase the large dimensions of the ring, 54 Å from the X-ray structure of the K_{10} ring³⁶, and the observation of 10 cardiolipins in complex with the ring, together with measurements from quantitative lipidomics, are consistent with stoichiometric binding of one lipid per K subunit. This leads to a model in which 10 cardiolipins bind to the membrane ring, adapting the central cavity for efficient rotation of the C subunit by reducing the orifice to 38 Å, very similar to that modelled for the six fold symmetric ring of *Tt*ATPase (39 Å).

Table 1

The total number of basic charges for the series of membrane complexes considered here was computed together with the number of basic residues in the transmembrane regions. The most likely location of protonated sites was deduced from the total number of basic residues in the membrane and soluble proteins using MD simulations in vacuum. The number of charges, determined from mass spectra, was assigned to the protonation sites that maintained the most stable structures. The average charge state observed in the electrospray spectrum is also shown.

	total basic residues	basic residues in TM region	charged residues in TM region	average charge state
BtuCD	142	10	0	22.8
CL12	74	0	0	22.2
EmrE	10	1	0	8
Kirbac	184	0	0	25.3
LmrA	116	0	0	18.9
LmrCD	129	2	0	25
MexB	242	18	3	39.9
MtrE	174	3	3	25